Environ. Sci. Technol. **2002**, *36,* 3936−3944

Evaluation of the Efficiency of Photodegradation of Nitroaromatics Applying the UV/H_2O_2 Technique

FERNANDO S. GARCÍA EINSCHLAG, JORGE LOPEZ, LUCIANO CARLOS, AND ALBERTO L. CAPPARELLI*

Instituto de Investigaciones Fisicoquímicas Teóricas y Aplicadas (INIFTA), Departamento de Química, Facultad de Ciencias Exactas, Universidad Nacional de La Plata, Casilla de Correo 16, Sucursal 4, (1900) La Plata, Argentina

ANDRÉ M. BRAUN AND ESTHER OLIVEROS*

Lehrstuhl für Umweltmesstechnik, Engler-Bunte-Institut, Universität Karlsruhe, D-76128 Karlsruhe, Germany

Photolysis of nitroaromatic compounds in aqueous solution is a very slow and inefficient process. As already observed for a variety of organic pollutants, considerably faster degradation rates of nitrobenzene (NBE), 1-chloro-2,4-dinitrobenzene (CDNB), 2,4-dinitrophenol (DNP), and 4-nitrophenol (PNP) could be achieved, when the oxidative degradation of these compounds was initiated by hydroxyl radicals produced by UV-C photolysis of H_2O_2. Analysis of intermediate products formed during irradiation by HPLC and IC showed that cleavage of the aromatic ring should occur at an early stage of the oxidation process and that organic nitrogen was almost completely converted to nitrate. The optimal initial concentration of hydrogen peroxide ($[H_2O_2]_{OPT}$) leading to the fastest oxidation rate, which depends on the initial substrate concentration ($[S]_0$), could be evaluated using a simplified expression based on the main reactions involved in the first stages of the degradation process. Using only a minimum of kinetic and analytical information, this expression shows that the ratio R_{OPT} (= $[H_2O_2]_{OPT}/[S]_0$) is related to the bimolecular rate constants for the reactions of hydroxyl radicals with substrate (k_S) and H_2O_2 (k_{HP}) and to the corresponding molar absorption coefficients (ϵ_S, ϵ_{HP}). Competition experiments between selected pairs of the substrates showed that their relative reactivity toward hydroxyl radicals could be correctly predicted using the same simplified approach. The results of our investigations as well as literature data support the general validity of the proposed procedure for optimizing oxidation rates of the UV/H_2O_2 process.

Introduction

Chemical remediation of wastewaters is one of the main aspects in modern environmental chemistry. Biological treatment uses microorganisms to metabolize the pollutants, a technique broadly applied to the treatment of wastewater from urban areas. However a large number of compounds are not biodegradable or cannot be destroyed by biological treatment due to their toxicity. Research on alternative or additional methods of wastewater treatment is of current interest and has led already to the development of photochemical processes for the oxidative degradation of pollutants in aqueous solution. In general, the use of UV/visible radiation can lead to the degradation of organic pollutants by two main processes (*1*): (I) excitation of the substrate and its subsequent decomposition (photolysis) and (II) generation of highly oxidizing species able to attack the substrate. The latter is primarily based on the generation of hydroxyl radicals (Advanced Oxidation Procedures (AOP) (*1*−*3*) and include UV/H_2O_2 (*1, 2, 4*), UV/TiO_2 (*3*), UV/H_2O_2/O_3 (*5*), UV/H_2O_2/Fe(II) or Fe(III) (photoassisted Fenton reaction) (*6*), and VUV photolysis of water (*7*), among others.

In the UV/H_2O_2 process, photolysis of H_2O_2 results in the homolysis of the oxygen−oxygen bond and the production of hydroxyl radicals (HO•). This technique presents a series of advantages (*2, 8*): (a) HO• radicals are highly reactive species, (b) H_2O_2 can be readily mixed with water in all proportions, (c) costs associated to production and handling of H_2O_2 are smaller than the corresponding ones for e.g. ozone. The process leads in most cases to the mineralization of the organic substrate, i.e. to the production of CO_2, water, and mineral acids (when the substrates contain heteroatoms). It should be noted, however that complete mineralization by the UV/H_2O_2 process may be an uneconomical goal for treatment and would not be required when intermediate products are nontoxic and biodegradable.

The UV/H_2O_2 method has been applied to the degradation of a variety of pollutants (*1, 2, 4, 8*−*12*). Experimental results show that the efficiency of the process strongly depends on the initial concentrations of substrate and additive as well as on the chemical structure of the substrate. Hydroxyl radicals react by addition to aromatic substrates and by hydrogen abstraction from aliphatic compounds, yielding carbon centered radicals. The latter add molecular oxygen and the resulting peroxyl radicals undergo further thermal reactions, leading eventually to substrate mineralization (*13, 14*).

In a previous study on the photodegradation of 4-chloro-3,5-dinitrobenzoic acid (CDNBA) (*2*) using the UV/H_2O_2 technique, we have proposed a simple method for predicting the amount of H_2O_2 leading to the highest degradation efficieny. However, the analysis was restricted to one compound, and a more general application of this method remained to be tested. In this work we analyze the effect of H_2O_2 and substrate concentrations on the efficiency of the UV/H_2O_2 technique and correlate the optimal conditions for the process with the absorption characteristics of the substrates and with their reactivity toward HO•. Four nitroaromatic compounds were chosen as model substrates: 1-chloro-2,4-dinitrobenzene (CDNB), 2,4-dinitrophenol (DNP); 4-nitrophenol (PNP), and nitrobenzene (NBE). Previous results on CDNBA (*2*) were used for comparison.

Experimental Section

Chemicals. 1-Chloro-2,4-dinitrobenzene (99%, *Aldrich*), 2,4-dinitrophenol (99%, *Riedel de Häen*), 4-nitrophenol (99%, *Fluka* and *Riedel de Haën*), and nitrobenzene (95%, *May&Baker*) were used without further purification for preparing aqueous solutions containing 15−200 mg L^{-1} of substrate. Unless otherwise indicated, the initial pH was adjusted to 2.5 using H_2SO_4 (Merk). Dissolution of the organic compounds was facilitated by sonication (when required, solutions were cooled in order to avoid heating induced by ultrasonic waves). Concentrations of H_2O_2 (*30% Perhydrol,*

* Corresponding author phone: +49 721 608 2557; fax: +49 721 608 6240; e-mail: Esther.Oliveros@ciw.uni-karlsruhe.de.

10.1021/es0103039 CCC: $22.00
Published on Web 08/13/2002

Merck) ranged from 5.5×10^{-3} to 0.6 M. Water was of Milli-Q quality. 4-Chloro-2,5-dinitrobenzoic acid (*Aldrich*) was also employed in competition experiments. This substance was previously purified as already described (*2*).

All other chemicals used were ACS grade. H_2O_2 (30% w/w in H_2O), H_2SO_4, H_3PO_4, $KMnO_4$, triethanolamine (TEA), oxalic acid, formic acid, acetonitrile, and acetic acid were purchased from *Merck*. H_2O_2 was analyzed by the classic $KMnO_4$-titration.

Absorbance Measurements. Absorption spectra were registered on a double beam *Cary 3* spectrophotometer. Measurements were made using quartz cells of 0.2 cm optical path length.

HPLC Measurements. HPLC analyses were carried out using an *HP1100 Ti-series* equipment with a *LiChrospher 100 RP-18* column (length: 125 mm, diameter: 4 mm, film thickness: 5 mm); the eluent was a mixture of acetonitrile and water (40/60). The aqueous phase contained 3.75 mL of TEA and 2 mL of H_3PO_4 dissolved in 1 L of water. A flow rate of 1 mL/min was used. Calibration curves for CDNB, DNP, PNP, and NBE were established under identical conditions.

Ionic Chromatography. IC measurements of inorganic and organic anions were performed on a *DIONEX DX500* series equipment using an *IONPAC AS14 DIONEX* column (length: 240 mm, diameter: 4 mm); an aqueous solution (pH 10) of Na_2CO_3 (2.7×10^{-3} M) and $NaHCO_3$ (3×10^{-4} M) was employed as eluent at a flow rate of 1.2 mL/min. The presence of cations, such as NH_4^+, was investigated using a *DIONEX CD12* column (length: 240 mm, diameter: 4 mm); the mobile phase was an aqueous solution of methanesulfonic acid at a flow rate of 1.0 mL/min. Calibration curves were established for all ionic species investigated.

Other Measurements. Dissolved organic carbon (DOC) was analyzed with a *Beckman Tocamaster 915-B* equipment (oven temperature 950 °C). The experimental error on DOC values was ±8%. The pH of the irradiated solutions was determined using a *PHM220 Radiometer* pH meter. Selective electrodes (*Radiometer F1012Cl* and *ISE25NO3*) were used to determine Cl^- and NO_3^- concentrations. Calomel and Ag/AgCl electrodes were used as reference electrodes. Organic compounds where previously extracted from aqueous samples with isooctane in order to avoid adsorption of nitrocompounds on the PVC selective membrane.

Photochemical Reactors. The experiments were performed in two annular photochemical reactors (Nr 1326, *DEMA, Mangels*, Bornheim-Roisdorf, Germany). The reactors are similar but they have different capacities. One of them had a volume of 750 mL (internal radius = 2.0 cm, external radius = 4.0 cm and height = 20.0 cm) and was equipped with a medium-pressure Hg arc (*Philips HPK 125 W*), positioned in the axis of the reactor in a quartz well. The second reactor had a capacity of 800 mL (internal radius = 2.5 cm, external radius = 4.0 cm and height = 26.0 cm) and was operated with a medium-pressure Hg lamp TQ 150 (150 W) from *Heraeus Nobelight* (Hanau, Germany). The spectral distribution of the emission of this lamp has been published elsewhere (*15*). The photon fluxes entering the reactors were 9.8×10^{-6} einstein s^{-1} (HPK 125) and 1.2×10^{-5} einstein s^{-1} (TQ 150) in the wavelength range 200−450 nm, as estimated from potassium ferrioxalate actinometry and the spectral emission profiles of the lamps (*6*). The reactors were equipped with ports for sample withdrawing. The purging gas was introduced from below through a glass frit. Solutions were continuously purged with synthetic air (21% O_2 in N_2), and the temperature was maintained at 25 °C (±1 °C) and 21 °C (±1 °C) for the experiments performed in the first and the second reactor, respectively. H_2O_2 was added to the reaction system just before starting the irradiation.

Results

UV Photolysis. Aqueous solutions of CDNB, DNP, NBE, and PNP were photolyzed at pH 2.5 in the *DEMA* reactor using the HPK 125 lamp (Experimental Section). In all cases, no significant changes in the absorption spectra could be detected during irradiation (not shown). Less than 4% of the substrates were degraded under continuous irradiation for 2−3 h in the absence of H_2O_2.

Oxidative Photodegradation in the Presence of H_2O_2: Intermediate and Final Products. Dramatic changes were observed in the absorption spectra of aqueous solutions of CDNB, DNP, NBE, and PNP during irradiation in the presence of H_2O_2, as shown in Figure 1 for selected runs. The absorbance decrease indicates that the four nitroaromatic substrates are rapidly consumed under these conditions.

Substrates, intermediate, and final products were analyzed using HPLC and IC techniques. As an example, IC results for CDNB at different irradiation times are shown in Figure 2. In all cases, formate, oxalate, NO_2^- (traces), Cl^-, and NO_3^- anions were detected as intermediate and final products. PO_4^{3-} and SO_4^{2-} were observed at constant concentrations in all the samples. The presence of SO_4^{2-} results from initial pH adjustment using H_2SO_4, whereas small concentrations of PO_4^{3-} might be due to a possible contamination during dilution. DOC and electrochemical determinations (for Cl^- and NO_3^-) were also carried out.

Concentration profiles of substrates, intermediate, and final products analyzed in irradiated solutions in the presence of H_2O_2 are shown in Figure 3 for selected runs. Note that experimental conditions differ from one compound to another, and, therefore, concentration profiles cannot be directly compared (relative oxidation efficiencies are discussed below in the section on "Competitive photodegradation").

The following general remarks hold for the four compounds investigated (Figure 3): (a) complete depletion of substrates could be achieved; (b) formation of organic oxidation products (such as formic acid and oxalic acid) and inorganic ions (Cl^-, NO_3^-, NO_2^-) was observed; (c) concentrations of formic and oxalic acids reached maximum values and then decreased due to further oxidation to CO_2; formic acid reached its highest concentration before or when the substrate was completely oxidized, whereas the maximum concentration of oxalic acid was observed at longer irradiation times; (d) the pH value of the solution decreased during photolysis; (e) the amount of NO_3^- formed was almost stoichiometric in relation with the total initial nitrogen content; (f) DOC measurements showed that complete mineralization can be achieved only after relatively long irradiation times; (g) carbon and nitrogen balances suggest that, during the degradation process, some organic intermediates in addition to those mentioned above were formed but not always detected by the applied analytical methods. This might be of importance in applications: toxicity controls would be required when treatment is not carried out until complete mineralization is achieved (most cases), as some of the organic intermediates could be biocidal.

In the case of CDNB (Figure 3a), the organic chlorine was quantitatively released from the substrate as chloride anion. The rate of Cl^- production was coincident with the rate of substrate depletion. This result strongly suggests that the carbon−chlorine bond was cleaved during the initial stages of the process. A similar behavior was reported for CDNBA (*2*). NO_2^- was generated during the first minutes of irradiation (not shown), but its concentration was very low (less than 1.5×10^{-5} M) and dropped below the detection limit as soon as the substrate was completely depleted. Most probably, organic nitrogen was released as NO_2^- in the early stages of the photolysis, but was rapidly oxidized to NO_3^- in the strongly

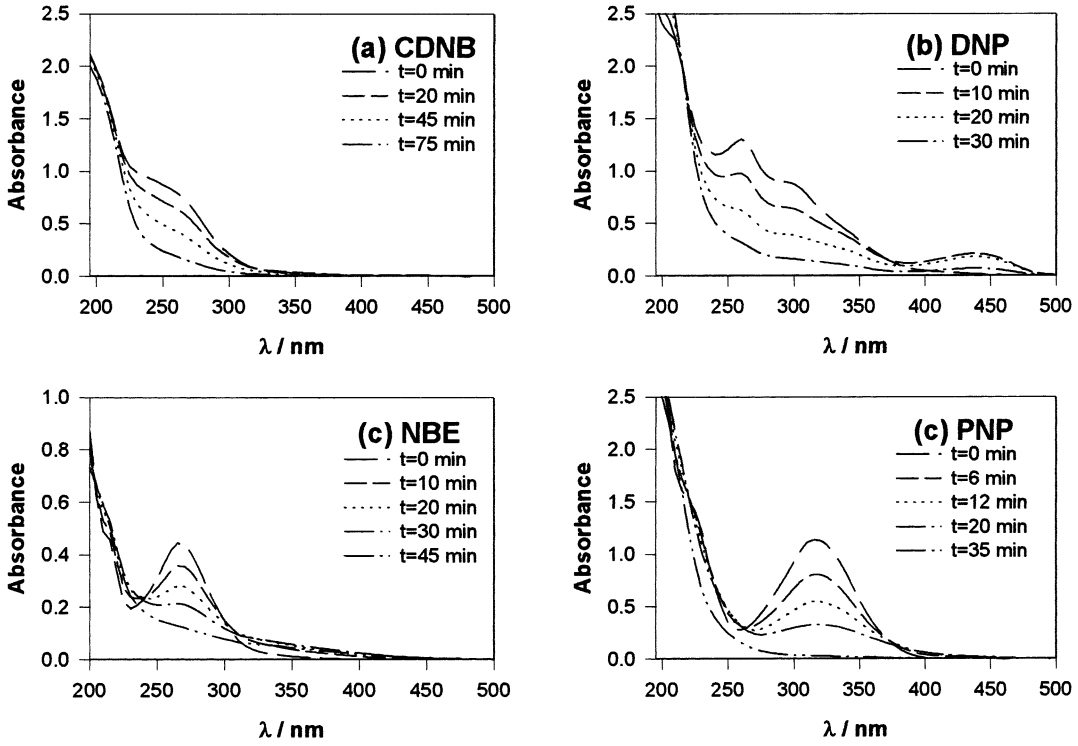

FIGURE 1. Absorption spectra of aqueous solutions of the nitroaromatic derivatives investigated in the presence of H_2O_2 at different irradiation times (initial concentrations: (a) CDNB: 2.9×10^{-4} M, H_2O_2: 0.034 M; (b) DNP: 5.0×10^{-4} M, H_2O_2: 0.045 M; (c) NBE: 2.9×10^{-4} M, H_2O_2: 5.5×10^{-3} M; and (d) PNP: 5.8×10^{-4} M, H_2O_2: 4.5×10^{-3} M; optical path length of spectroscopic cell: 0.2 cm; initial absorbance in photoreactor (optical thickness: 2.25 cm) > 2 below 320 nm).

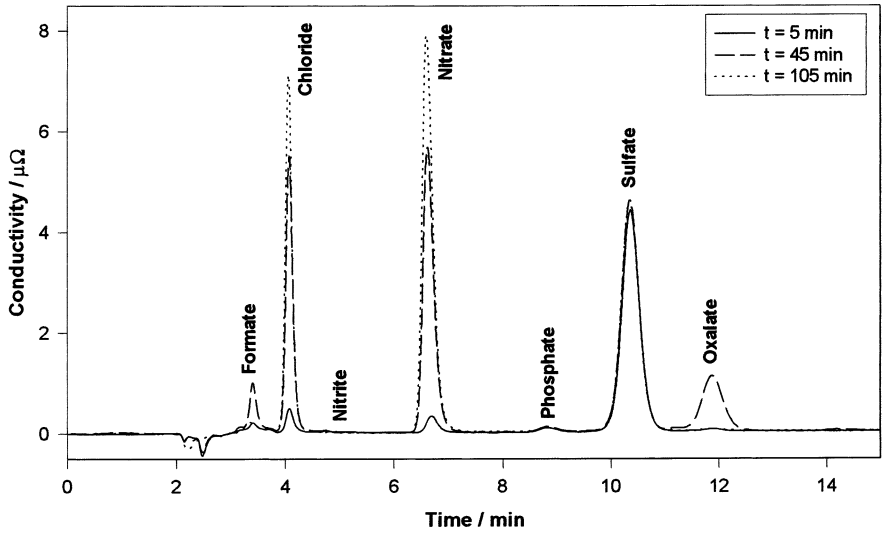

FIGURE 2. Ion chromatography profiles for the photodegradation of CDNB in aqueous solution in the presence of H_2O_2 (initial concentrations: CDNB: 5.2×10^{-4} M, H_2O_2: 0.044 M).

oxidizing medium. The initial rate of formic acid generation was approximately 2.2 times higher than the rate of substrate oxidation. Therefore at least two molecules of formic acid were produced per molecule of substrate. In the case of DNP (Figure 3b), the initial rate of formation of formic acid relative to substrate depletion was slower than for CDNB, and the maximum concentration of formic acid was observed when the substrate was completely depleted. For the dinitro aromatics, CDNB and DNP (Figure 3a,b), the amount of NO_3^- produced corresponds to the stoichiometric molar ratio of 2/1 that would be expected if all the organic nitrogen content was mineralized to NO_3^- ($2NO_3^-$ anions formed per molecule of substrate mineralized).

In the case of NBE, besides production of NO_3^-, formate, and oxalate (Figure 3c), 2-nitrophenol, 3-nitrophenol, and 4-nitrophenol were formed (detected by HPLC, not shown). These intermediates were subsequently oxidized, and, under the experimental conditions shown in Figure 3c, the rate of production of NO_3^- was 30% smaller than that observed for substrate depletion. The relative amounts of the intermediate nitrophenols are in agreement with the expected reactivity of hydroxyl radicals in their electrophilic attack at the aromatic ring of NBE. Under similar experimental conditions, oxidative degradation of PNP was faster than that of the other compounds investigated. Formation of formic and oxalic acids was however delayed in comparison with the other

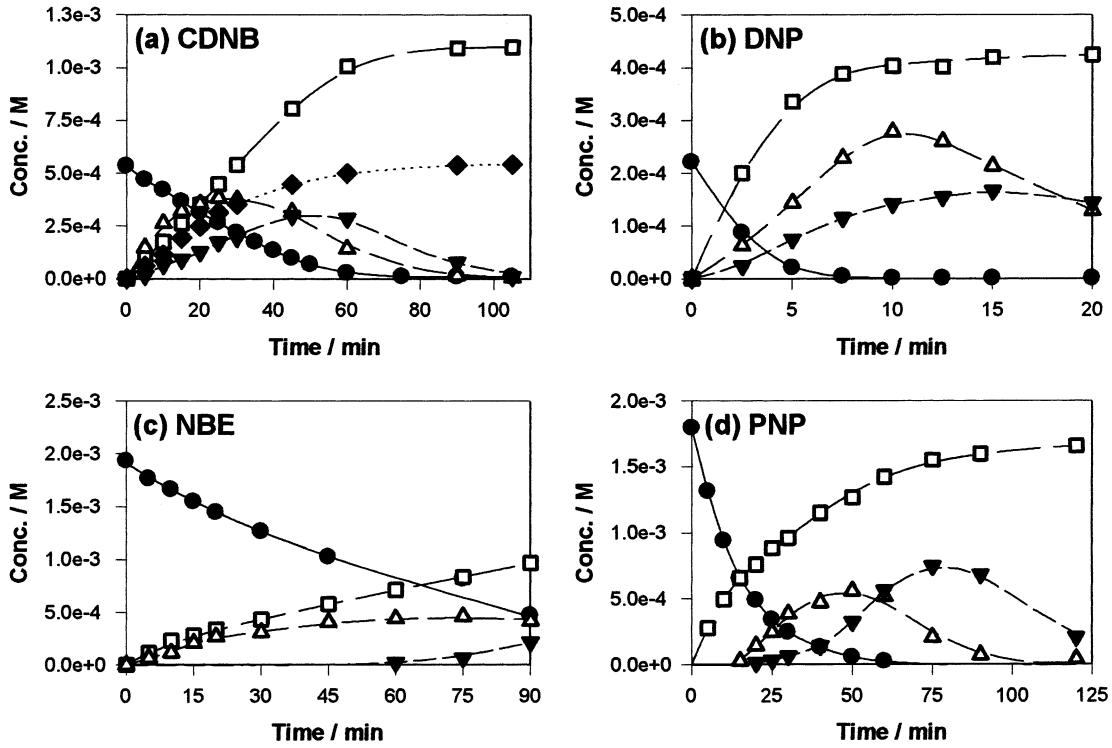

FIGURE 3. Concentration profiles for irradiated solutions of the nitroaromatic derivatives investigated in the presence of H_2O_2: *filled circles*: substrates, *squares*: nitrate, *open triangles*: formate, *filled triangles*: oxalate, *diamonds*: chloride (initial concentrations: (a) CDNB: 5.2×10^{-4} M, H_2O_2: 0.044 M; (b) DNP: 2.2×10^{-4} M, H_2O_2: 0.044 M; (c) NBE: 1.9×10^{-3} M, H_2O_2: 0.011 M; and (d) PNP: 1.8×10^{-3} M, H_2O_2: 0.022 M; initial pH = 2.50).

compounds (Figure 3d). For the two mononitro derivatives (NBE and PNP), NO_3^- production was significantly slower than substrate depletion (Figure 3c,d), but at longer irradiation times when mineralization was achieved, stoichiometric formation of NO_3^- was observed, as in the case of CDNB and DNP.

More investigations aiming at the identification of all organic intermediates would be necessary before a detailed mechanistic scheme can be proposed for the oxidation of nitroaromatic compounds by the UV/H_2O_2 process. It should be noted however that the results presented in this work and those obtained previously for CDNBA (*2*) show that Cl^- and NO_3^- are produced almost stoichiometrically with respect to the initial chlorine and nitrogen contents of the substrates. This result may be explained by a mechanism involving electrophilic attack of HO$^\bullet$ on a carbon atom substituted by Cl (or NO_2) followed by HCl (or HNO_2) elimination. It has been already shown that the addition of HO· may take place at various sites of an aromatic nucleus (*4*). In most cases, cleavage of the aromatic ring should occur at an early stage of the oxidation process, as indicated by the early release of formic acid (Figure 3). It is worthwhile to note that (i) hydroxylated aromatic intermediates were only detected in substantial amounts in the case of NBE, a monosubstituted aromatic compound; (ii) formation of NO_3^- was delayed with respect to substrate depletion for the less substituted derivatives, NBE and PNP, where more positions on the aromatic ring are available for addition of HO·; and (iii) depending on their structure, some of the aromatic intermediates might be rapidly depleted and be present only at very low concentrations.

Oxidative Photodegradation in the Presence of H_2O_2: Oxidation Rates. The effect of the initial H_2O_2 concentration on the efficiency of the UV/H_2O_2 process was analyzed in a series of experiments using different initial concentrations of substrates ($[S]_0$) ranging from 15 to 100 mg L^{-1}. The concentration of H_2O_2 was varied in a wide range depending on the nature of the substrate (e.g., in the case of CDNB, from 3.3×10^{-3} up to 3.5×10^{-1} M). Initial rates of substrate disappearance ($r = -d[S]/dt$) under different conditions were determined. In all cases, when increasing the concentration of H_2O_2, a maximum rate (r_{max}) could be observed (Figure 4). A similar trend was also reported for CDNBA (*2*) and for a variety of aromatic and aliphatic compounds [see e.g. refs *8* and *16*−*18*]. When increasing the initial substrate load $[S]_0$, the optimal H_2O_2 concentration ($[H_2O_2]_{OPT}$, defined as the initial H_2O_2 concentration for which r_{max} was reached) increased proportionally. Figure 4 shows the behavior of the normalized initial rates of oxidation (r/r_{max}) under different experimental conditions. In these plots, r/r_{max} is represented as a function of the parameter $\boldsymbol{R}$ (defined as $[H_2O_2]_0/[S]_0$), for each nitroaromatic derivative investigated. It is worthwhile to mention that optimal concentration ratios $\boldsymbol{R_{OPT}}$ ($=[H_2O_2]_{OPT}/[S]_0$) were independent of $[S]_0$ and of the reaction volumes used in these experiments.

The analysis of the shape of the curves reveals a marked asymmetry. As the initial concentration of H_2O_2 increases for a given $[S]_0$, a dramatic change in the initial oxidation rate can be observed, but when $\boldsymbol{R} > \boldsymbol{R_{OPT}}$, this rate shows a smooth decrease (Figure 4). This behavior is of great importance from both a practical and an economical point of view, since there is a wide range of $\boldsymbol{R}$ values corresponding to oxidation rates of at least 90% of the optimal rate. DOC depletion and NO_3^- production rates show similar $\boldsymbol{R_{OPT}}$ values, within experimental error.

Discussion

Simplified Mechanism of Oxidative Photodegradation. The degradation of pollutants by the UV/H_2O_2 technique is initiated by the attack of HO$^\bullet$ radicals generated by photolysis of H_2O_2. Hydroxyl radicals may react with the substrate, H_2O_2, and with the intermediate products of the degradation process. From the initial oxidation of the substrate until

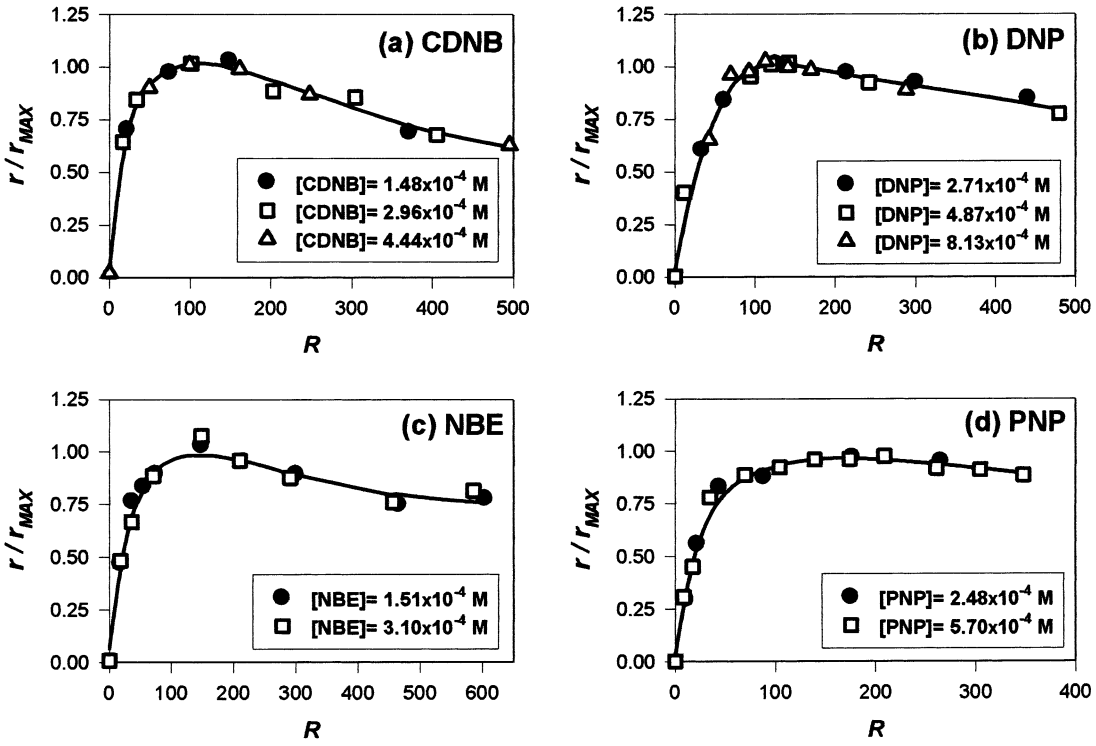

FIGURE 4. Normalized initial rates of substrate disappearance r/r_{max} vs R (=$[H_2O_2]_0/[S]_0$) for the photodegradation of CDNB, DNP, NBE, and PNP in aqueous solution in the presence of H_2O_2.

complete depletion, a complex set of reactions takes place, where other oxidizing species (e.g. hydroperoxyl radical ($HO_2^{\bullet}$), nitrogen containing radicals) might participate in the reaction mechanism (*10, 19*), and a detailed analysis of all the reactions involved in the manifold of oxidative degradation is very complex (*8, 10, 11, 20, 21*). However, the general trends observed for the different substrates are very similar under all experimental conditions applied. Hence a simple kinetic model for describing the observed behavior for the initial oxidation rates of all substrates tested might be found.

During the initial stages of the oxidation process, only substrate and H_2O_2 are present in substantial amounts, and the following main reactions may be considered (*8, 9, 12*)

$$H_2O_2 + h\nu \rightarrow 2HO^{\bullet} \quad I_{HP}\Phi_{HP} \qquad \text{(A)}$$

$$H_2O_2 + HO^{\bullet} \rightarrow HO_2^{\bullet} + H_2O \quad k_{HP} \qquad \text{(B)}$$

$$S + h\nu \rightarrow \text{Int} \quad I_S\Phi_S \qquad \text{(C)}$$

$$S + HO^{\bullet} \rightarrow \text{Int} \quad k_S \qquad \text{(D)}$$

where I_{HP} and I_S are the rates of photons absorbed by H_2O_2 and by the substrate, respectively, Φ_{HP} and Φ_S are the quantum yields of respective photolyses, and k_{HP} and k_S are the bimolecular rate constants for the corresponding reactions with hydroxyl radicals.

In this reaction scheme, reactions implying $HO_2^{\bullet}$ or $O_2^{-\bullet}$ radicals have not been considered, as their reactivity is much lower than that of $HO^{\bullet}$ (*22*−*25*). A similar remark applies to the reactions associated with the intermediate products (Int), whose concentrations during the first minutes of irradiation may be neglected. At this point a comment related to the use of H_2SO_4 for adjusting the initial pH of the solutions seems necessary. The reaction of $HO^{\bullet}$ with HSO_4^- generates $SO_4^{-\bullet}$ radicals, which are able to react with organic substrates and may introduce alternative reaction pathways. Control experiments in the absence and presence of H_2SO_4 did not yield significant differences. This result may be explained by the relatively low reactivity of $HO^{\bullet}$ toward HSO_4^- ($k = 3.5 \times 10^5$ M^{-1} s^{-1} (*26*)). Consequently, the results discussed below refer indistinctly to experiments in the presence or in the absence of H_2SO_4.

Considering the simplified mechanism proposed, the rate of substrate consumption (r) is given by the sum of the rates of reactions (C) and (D):

$$r = \frac{-d[S]}{dt} = I_S\Phi_S + k_S[S][HO^{\bullet}] \qquad (1)$$

In a solution where several species absorb radiation at the same wavelengths, the total number of photons absorbed is the sum of the photons absorbed by each species (*27, 28*). If Lambert−Beer's law holds under the present experimental conditions, the rate of photons absorbed by the substrate (I_S) at a given wavelength of irradiation is given by

$$I_S = I_0(1 - 10^{-A})\frac{\epsilon_S c_S}{\epsilon_{HP}c_{HP} + \epsilon_S c_S} \qquad (2)$$

where I_0 is the incident photon rate (einstein L^{-1} s^{-1}), $\epsilon_S c_S/(\epsilon_{HP}c_{HP} + \epsilon_S c_S)$ is the fraction of photons absorbed by the substrate, ϵ_S and ϵ_{HP} are the molar absorption coefficients of substrate and H_2O_2, respectively (M^{-1} cm^{-1}), c_S and c_{HP} are the corresponding concentrations (M), and A (= $\Sigma\epsilon_i c_i d$) represents the total absorbance of the solution (d: optical path length).

The steady-state concentration of $HO^{\bullet}$ radicals is given by eq 3

$$[HO^{\bullet}] = \frac{r_{HO}}{k_{HP}c_{HP} + k_S c_S} \qquad (3)$$

where r_{HO} is the rate of $HO^{\bullet}$ production.

In the UV/H_2O_2 process, the main path for the generation of $HO^{\bullet}$ radicals is the photodissociation of H_2O_2. The quantum

yield of photolysis of H_2O_2 (Φ_{HP}) is approximately 0.5 in the wavelength range from 200 to 300 nm (*29*). The rate of HO$^\bullet$ production (r_{HO}) may be expressed as

$$r_{HO} = \frac{2I_0\Phi_{HP}(1 - 10^{-A})\epsilon_{HP}c_{HP}}{\epsilon_{HP}c_{HP} + \epsilon_S c_S} \quad (4)$$

where $\epsilon_{HP}c_{HP}/(\epsilon_{HP}c_{HP} + \epsilon_S c_S)$ is the fraction of photons absorbed by H_2O_2.

Combining eqs 1−4 and under conditions where the absorbance of the solution is greater than 2, the oxidation rate of the substrate (r) may be expressed as

$$r = \frac{I_0}{\epsilon_{HP}\boldsymbol{R} + \epsilon_S}\left\{\Phi_S\epsilon_S + \frac{2\Phi_{HP}k_S\epsilon_{HP}\boldsymbol{R}}{k_{HP}\boldsymbol{R} + k_S}\right\} \quad (5)$$

where $\boldsymbol{R} = [H_2O_2]_0/[S]_0$ (see results).

The optimal ratio $\boldsymbol{R_{OPT}}$ leading to the highest initial oxidation rate can be obtained by differentiation of eq 5 (i.e. $\boldsymbol{R} = \boldsymbol{R_{OPT}}$ for $dr/d\boldsymbol{R} = 0$)

$$\boldsymbol{R_{OPT}} = \frac{\sqrt{4\Phi_{HP}{}^2\epsilon k + 2\Phi_{HP}\Phi_S(k^2 - \epsilon k)} - 2\Phi_S k}{k(2\Phi_{HP}\epsilon + \Phi_S k)} \quad (6)$$

where $\epsilon = \epsilon_{HP}/\epsilon_S$ and $k = k_{HP}/k_S$.

Equation 6 was obtained taking into account the initial rate of disappearance of the substrate by photolysis (reaction C) and by oxidative degradation initiated by HO$^\bullet$ radicals (reaction D). However, in most cases, reaction C can be neglected in the presence of H_2O_2. Moreover, the fraction of the incident photons absorbed by the substrate diminishes as R increases. Under these conditions, eq 5 simplifies to eq 7, and eq 6 gives eq 8.

$$r = \frac{2I_0\Phi_{HP}\epsilon\boldsymbol{R}}{(\epsilon\boldsymbol{R} + 1)\,(k\boldsymbol{R} + 1)} \quad (7)$$

$$\boldsymbol{R_{OPT}} = \sqrt{\frac{1}{k\epsilon}} = \sqrt{\frac{k_S\epsilon_S}{k_{HP}\epsilon_{HP}}} \quad (8)$$

This simple expression of $\boldsymbol{R_{OPT}}$ ($= [H_2O_2]_{OPT}/[S]_0$) might be used, either to evaluate $[H_2O_2]_{OPT}$ if k_S and ϵ_S at a given λ are known or to estimate k_S if $[H_2O_2]_{OPT}$ is determined experimentally. The validity of eqs 5−8 was tested by comparing experimental and simulated variations of the oxidation rates.

Simulation of the Rate of Substrate Consumption. The variation of the initial rate of substrate disappearance (r) as a function of $\boldsymbol{R}$ predicted by eq 5 is shown in Figure 5a for a hypothetical pollutant (irradiation at 254 nm). The following data were taken into account for the calculations: (i) quantum yields of photolysis of various aromatic compounds (Φ_S) have been determined to be between 10^{-3} and 10^{-4} (*2, 30*); (ii) molar absorption coefficients (ϵ_S) at 254 nm for the studied compounds are in the range between 5.4×10^3 and 1.4×10^4 M^{-1} cm^{-1} and rate constants for the reaction of HO$^\bullet$ with different aromatic compounds (k_S) are in the range 10^8−10^{10} M^{-1} s^{-1} (*31*); and (iii) the molar absorption coefficient of H_2O_2 (ϵ_{HP}) at 254 nm is 18.7 M^{-1} cm^{-1} (*29*) and the rate constant for the bimolecular reaction between H_2O_2 and HO$^\bullet$ radicals (k_{HP}) has a value of 2.7×10^7 M^{-1} s^{-1} (*31*). The general trend predicted for r as represented in Figure 5a is in very good agreement with the varations of r observed experimentally for the four nitroaromatic derivatives investigated (Figures 4a−d) as well as with results previously reported for the degradation of CDNBA (*2*) and a variety of aromatic and aliphatic compounds (*8, 16*−*18*).

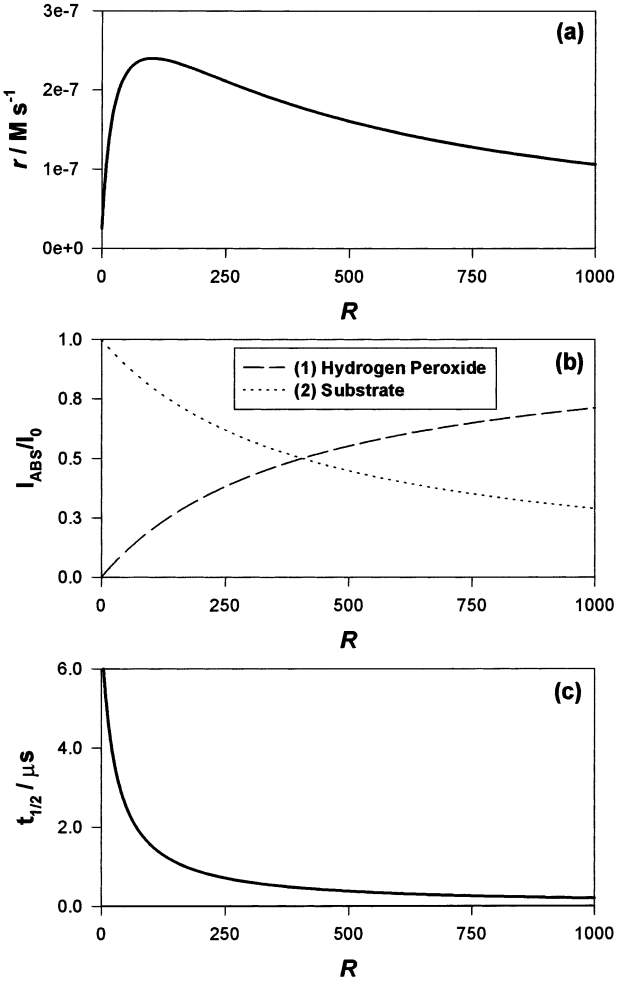

FIGURE 5. Simulation of (a) initial rate of substrate disappearance (r) using eq 6, (b) initial fraction of photons absorbed by the substrate and by H_2O_2 (I_{ABS}/I_0), and (c) half-life of HO$^\bullet$ radicals ($t_{1/2}$, eq 9) as a function of R for a hypothetical pollutant ($\Phi_S = 10^{-3}$, $\epsilon_S = 7500$ M^{-1} cm^{-1}, $k_S = 1.0 \times 10^9$ M^{-1} s^{-1}, wavelength of irradiation: 254 nm).

In fact, in the presence of H_2O_2, consumption of the substrate by photolysis (reaction C) is negligible, and eq 7 may be used instead of eq 5 for the simulations. On the basis of eq 7, the trend observed for the variation of the initial rate of substrate disappearance (r) as a function of $\boldsymbol{R}$ may be qualitatively explained. This equation indicates that, for a given substrate and a given experimental design (reactor volume, geometry, incident photon rate, etc.), r depends only on the ratio $\boldsymbol{R}$ ($=[H_2O_2]_0/[S]_0$). Therefore solutions with different initial pollutant concentrations but with the same value of $\boldsymbol{R}$ should have the same initial rate of disappearance. Moreover, eq 7 shows that the variation of r as a function of $\boldsymbol{R}$ should exhibit a maximum, since r is the ratio of a first degree polynomial to a second degree polynomial (both in terms of parameter $\boldsymbol{R}$). For small values of $\boldsymbol{R}$, the linear term of the numerator will dominate, while for larger values, the quadratic term in the denominator will be more important (*2*). The observed behavior is due to two contradictory effects. On one hand, as the value of $\boldsymbol{R}$ increases, the fraction of photons absorbed by H_2O_2 increases (Figure 5b), leading to an increase in the production of HO$^\bullet$ radicals (reaction A). On the other hand, at high values of $\boldsymbol{R}$, reaction B (trapping of HO$^\bullet$ by H_2O_2) competes more effectively with reaction D (attack of the substrate by HO$^\bullet$). This latter effect can be also represented by the decrease of HO$^\bullet$ half-life ($t_{1/2}$, as defined

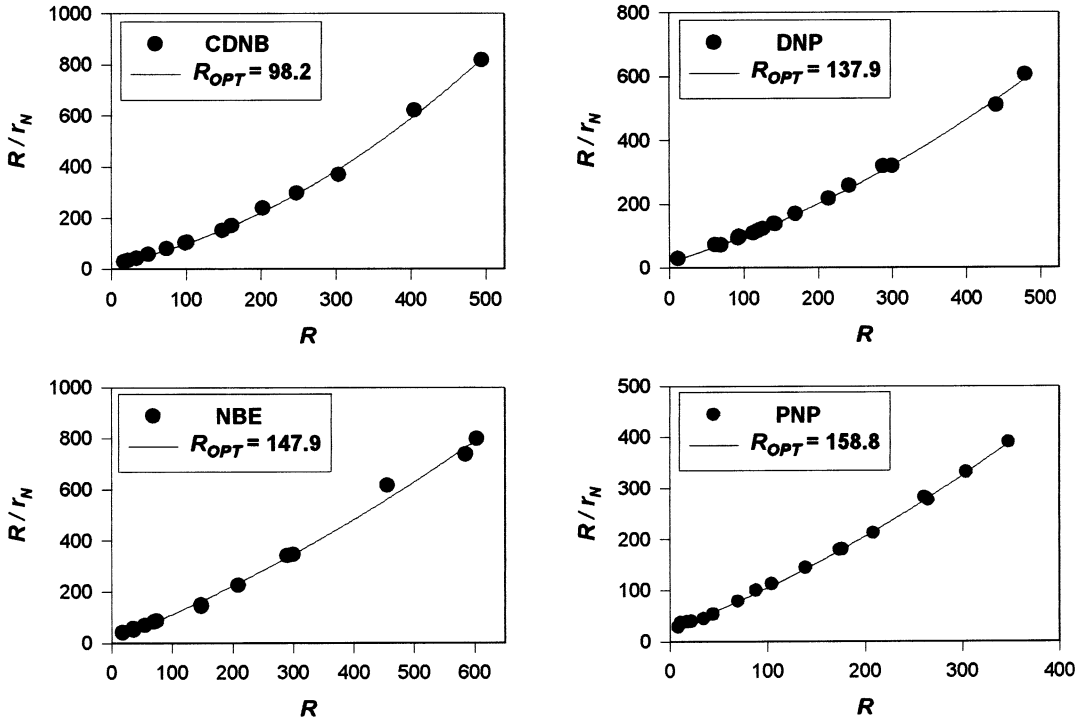

FIGURE 6. Plots of R/r_N vs R for the nitroaromatic derivatives investigated ($r_N = r/r_{max}$ is the normalized initial rate of substrate disappearance).

in eq 9, Figure 5c).

$$t_{1/2} = \frac{\ln(2)}{k_{HP}c_{HP} + k_S c_S} \quad (9)$$

Estimation of Experimental Values of R_{OPT}. When the rate constant of the reaction between a substrate and HO• (k_S) is not known, an estimate of k_S may be obtained using eq 8 if the value of R_{OPT} is experimentally determined from the experimental curves shown in Figure 4. Two different methods have been developed to estimate with good precision the values of R_{OPT}. The first method does not require any kinetic model and uses an algorithm that combines a Taylor series around each experimental point with polynomial regression analysis. The function obtained represents the behavior of the data in the whole experimental domain (Figure 4, solid lines), and the determination of the value of R_{OPT} is made by taking its numerical derivative (*32*). The second method uses the expression for the initial rate of substrate disappearance. After reordering eq 7, the following expression is obtained

$$\frac{R}{r} = aR^2 + bR + c \quad (10)$$

where $a = \epsilon k/(2I_0\Phi_{HP}\epsilon)$, $b = (\epsilon + k)/(2I_0\Phi_{HP}\epsilon)$, and $c = 1/(2I_0\Phi_{HP}\epsilon)$ are the coefficients of the polynomial function.

From the coefficients a and c, R_{OPT} is directly calculated as $(c/a)^{1/2}$. Figure 6 shows the variation of R/r_N ($r_N = r/r_{max}$: normalized initial rate) vs R for each substrate investigated. In all cases, the experimental behavior may be fitted by a quadratic polynomial as predicted by eq 10.

Table 1 shows the results obtained for R_{OPT} using both methods for the four studied compounds as well as for CDNBA (*2*). No significant differences were observed between both procedures.

Competitive Photodegradation. A quantitative description of the kinetics of photooxidation requires the knowledge of the rate constants of the reactions of HO• radicals with the substrate as well as with the intermediates of the degradation manifold. Absolute rate constants for the reactions of HO• with organic compounds are most often evaluated using pulse radiolysis or are obtained in some cases from EPR measurements. However, an evaluation of these rate constants is also possible by performing experiments where a given substrate competes for HO• radicals with a reference compound whose reactivity toward HO• is already known (*33*–*35*). To determine values of relative rate constants, competition experiments among pairs of the investigated substrates were carried out. Results obtained for the pair PNF-NBE are shown in Figure 7. The substrate disappearance follows first-order kinetics for both PNP and NBE (Figure 7, inset), as predicted by eq 1 if UV photolysis of the substrate is neglected.

Under these conditions, eq 1 can be rewritten as

$$\frac{-\mathrm{d[S]}}{\mathrm{d}t} = k_S[S][HO^\bullet] \quad (1a)$$

$$\frac{-\mathrm{d[R]}}{\mathrm{d}t} = k_R[R][HO^\bullet] \quad (1b)$$

where the subscripts R and S refer to the reference compound and the substrate investigated, respectively (in case of Figure 7, S = PNP and R = NBE).

The ratio β ($=k_S/k_R$) is equal to the ratio of the pseudo-first-order rate constants k_S' ($=k_S[HO^\bullet]$, eq 1a) and k_R' ($=k_R[HO^\bullet]$, eq 1b). β was calculated from the slopes of the plots of ln([S]) and ln([R]) as a function of irradiation time (see inset of Figure 7). In all cases investigated in this work,

TABLE 1. Values of R_{OPT} ($=[H_2O_2]_{OPT}/[S]_0$) Obtained from the Curves in Figures 4a–d by Two Different Methods: (A) Taylor Analysis around the Maximum and (B) Quadratic Approach (Eq 10)

substrate	method A	method B
DNP	134 ± 9	138 ± 9
CDNBA	57 ± 9	61 ± 7
CDNB	105 ± 18	98 ± 15
NBE	152 ± 13	148 ± 12
PNP	165 ± 7	159 ± 10

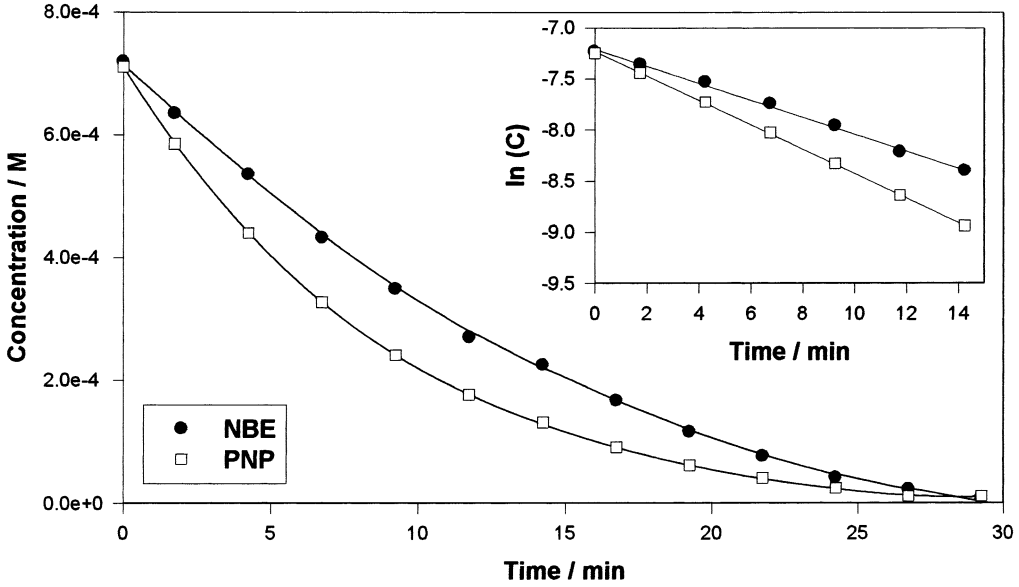

FIGURE 7. Concentration profiles obtained in a competition experiment using an aqueous solution containing 7.2 $\times$ 10^{-4} M of NBE and PNF ($[H_2O_2]_0 = 5.0 \times 10^{-2}$ M; concentrations of substrates determined by HPLC as described in the Experimental Section).

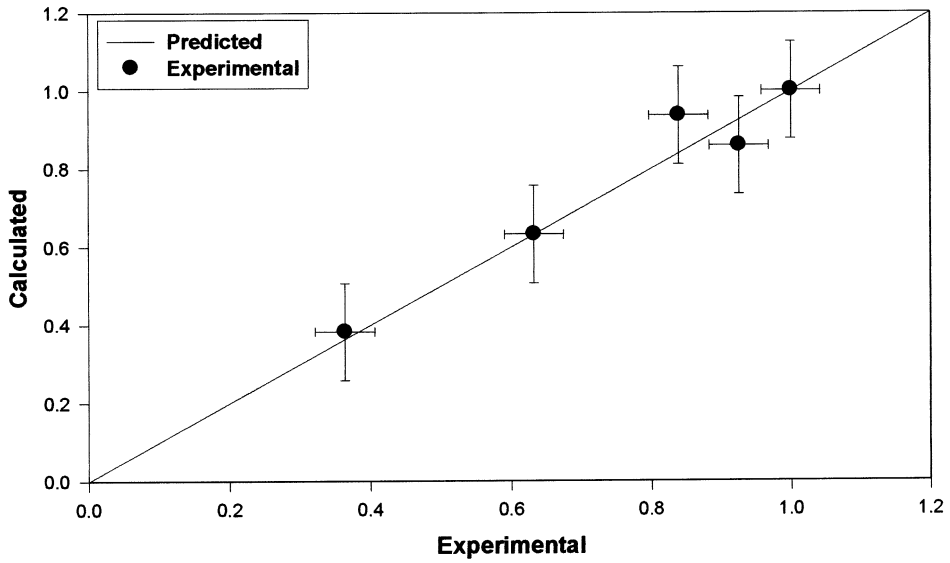

FIGURE 8. Comparison between experimental results of R^S_{OPT}/R^{PNP}_{OPT} (Table 1) and values calculated using eq 11 (see text).

pseudo-first-order oxidation rates were observed. The rate constants of the reaction of HO• radicals with PNP and NBE have been reported in the literature: $k_{PNP} = 3.8 \times 10^9$ M^{-1} s^{-1} and $k_{NBE} = 3.2 \times 10^9$ M^{-1} s^{-1} (*36*, *37*) (values measured the same year with the same technique), resulting in a value of β ($= k_{PNP}/k_{NBE}$) of 1.2. The experiments shown in Figure 7 give a value of 1.4 $\pm$ 0.2, in agreement with the literature value. β values for different pairs of substrates (including CDNBA) are shown in Table 2. Despite some data dispersion, the values listed show that the reactivity order toward HO• radicals for the substrates investigated is PNP > NBE > DNP > CDNB > CDNBA. This reactivity order is in agreement with that expected from the electrophilic nature of the hydroxyl radical and the electron-withdrawing or -donating substituents on the aromatic ring (*38*). It should be noted that, under the same experimental conditions and when $\boldsymbol{R} = \boldsymbol{R_{OPT}}$, the initial oxidation rates of the substrates investigated in this work follow the same order as the values of k_S. This is a consequence of the relative values of k_S and ϵ_S of the specific compounds investigated in this work. In general, for $\boldsymbol{R} = \boldsymbol{R_{OPT}}$, the initial rate of substrate oxidation (r_{max}) is obtained by combining eqs 7 and 8. When the behavior of

TABLE 2. Relative Rate Constants (β) of the Reaction with HO• for Different Couples of Nitroaromatic Derivatives Investigated

couple of substrates	β
PNP/NBE	1.4 $\pm$ 0.2
DNP/CDNB	2.7 $\pm$ 0.1
PNP/CDNB	9.5 $\pm$ 1.0
NBE/CDNB	6.1 $\pm$ 0.6
DNP/CDNBA	7.5 $\pm$ 0.5
CDNB/CDNBA	2.8 $\pm$ 0.2
PNP/CDNBA	26.9 $\pm$ 2.8
NBE/CDNBA	16.4 $\pm$ 1.4

r_{max} is dominated by the numerator of eq 7, r_{max} should be proportional to $(\epsilon/k)^{0.5}$ i.e. to $(k_S/\epsilon_S)^{0.5}$ and, if the values of ϵ_S are of the same order of magnitude, the ranking of r_{max} among the various substrates will be the same as the ranking of k_S.

Rate Constants for Reaction with Hydroxyl Radicals and $\boldsymbol{R_{OPT}}$. It is interesting to observe that the variation of $\boldsymbol{R_{OPT}}$ values among the different compounds is similar to that observed for the rate constants obtained in the competition

experiments. Equation 8 deduced from a simplified reaction scheme establishes that $\boldsymbol{R_{OPT}} = (k\epsilon)^{-0.5}$. This relation is only valid for a given wavelength of excitation. In fact, in the present study, polychromatic radiation sources were employed as is most often the case in technical applications. In this case, the spectral distribution of the radiation source as well as the molar absorption coefficients of substrate and H_2O_2 in the whole spectral range of absorption are required for a detailed study. In a simplified approach, we calculated an average molar absorption coefficient $<\epsilon_i>$ for each compound in the wavelength range of 230−255 nm and assumed that under polychromatic irradiation $\boldsymbol{R_{OPT}} \approx [k_S<\epsilon_S>/k_{HP}<\epsilon_{HP}>]^{0.5}$. To test this assumption, values of $<\epsilon_i>$ and of β (Table 2) were introduced in eq 11 for estimating $\boldsymbol{R^S_{OPT}/R^{PNP}_{OPT}}$. Experimental results (Table 1) and values calculated using eq 11 are compared in Figure 8. They are in good agreement within experimental error.

$$\sqrt{\beta_{S/PNP}\frac{\langle\epsilon_S\rangle}{\langle\epsilon_{PNP}\rangle}} \approx \frac{\boldsymbol{R^S_{OPT}}}{\boldsymbol{R^{PNP}_{OPT}}} \qquad (11)$$

where $\beta_{S/PNP} = k_S/k_{PNP}$.

Therefore a simple predictive model, useful in technical applications of the UV/H_2O_2 process, could be established.

Practical Implications. The results obtained for the nitroaromatic compounds investigated in this work as well as literature data (*2*, *8*, *16*−*18*) support the potential of the proposed approach to improve the efficiency of the UV/H_2O_2 process. The simplified mechanism for the oxidative photodegradation leads to very simple expressions (eqs 7 and 8) that describe well the experimental behavior observed (Figure 4). Equation 7 gives the oxidation rate as a function of the operating conditions (i.e. H_2O_2 and substrate concentrations), whereas eq 8 defines the optimal conditions that lead to the fastest rate. Since the variation of the oxidation rate is relatively flat around $\boldsymbol{R_{OPT}}$, there is a wide range of $\boldsymbol{R}$ values corresponding to oxidation rates of at least 90% of the optimal one. This range can be easily estimated using eqs 7 and 8 as design tools for technical development. When necessary, $\boldsymbol{R_{OPT}}$ (=$[H_2O_2]_{OPT}/[S_0]$) may be experimentally determined at the laboratory scale before implementing the process at the pilot or production level, since $\boldsymbol{R_{OPT}}$ does not depend on the reaction volume. Furthermore, the results shown in Figure 8 indicate that the model proposed may also be used when polychromatic radiation sources are employed, although a detailed analysis would require a rather complex mathematical treatment (*39*).

Acknowledgments

This work was supported in part by a project grant from the Agencia de Promoción Científica y Tecnológica de Argentina (ANPCyT Grant N° PICT 06-03531), the Consejo Nacional de Investigaciones Científicas y Tecnológicas (Grant No. PIP4354), and the University of La Plata (Project No. X-226). F.G.E. would like to thank the University of La Plata for a research graduate grant. A.L.C, F.G.E, A.M.B., and E.O. gratefully acknowledge support of the current cooperation program by SECyT (Secretaría de Ciencia y Técnica, Argentina) and BMBF (Bundesministerium fuer Bildung und Forschung, Germany).

Literature Cited

(1) Legrini, O.; Oliveros, E.; Braun, A. M. *Chem. Rev.* **1993**, *30*, 671−698.
(2) Lopez, J. L.; García Einschlag, F. S.; Gonzalez, M. C.; Capparelli, A. L.; Oliveros, E.; Hashem, T. M.; Braun, A. M. *J. Photochem. Photobiol., A: Chem.* **2000**, *137*, 177−184.
(3) Fujishima, A.; Rao, T. N.; Tryk, D. A. *J. Photochem. Photobiol., C: Photochem. Rev.* **2000**, *1*, 1−21.
(4) Ho, P. *Environ. Sci. Technol.* **1986**, *20*, 260−267.
(5) Glaze, W. H. *Environ. Sci. Technol.* **1987**, *21*, 224−230.
(6) Bossmann, S. H.; Oliveros, E.; Göb, S.; Siegwart, S.; Dahlen, E. P.; Payawan, L., Jr.; Straub, M.; Wörner, M.; Braun, A. M. *J. Phys. Chem. A* **1998**, *102*, 5542−5550, and references therein.
(7) Jakob, L.; Hashem, T. M.; Bürki, S.; Guindy, N. M.; Braun, A. M. *J. Photochem. Photobiol., A: Chem.* **1993**, *75*, 97−103.
(8) Stefan, M. I.; Hoy, A. R.; Bolton, J. R. *Environ. Sci. Technol.* **1996**, *30*, 2382−2390.
(9) Karpel Vel Leitner, N.; Gombert, B.; Ben Abdessalem, R.; Doré, M. *Chemosphere* **1996**, *32*, No. 5, 893−906.
(10) Stefan, M. I.; Bolton, J. R. *Environ. Sci. Technol.* **1998**, *32*, 1588−1595.
(11) Stefan, M. I.; Mack, J.; Bolton, J. R. *Environ. Sci. Technol.* **2000**, *34*, 650−658.
(12) Carter, S. R.; Stefan, M. I.; Bolton, J. R.; Safarzadeh-Amiri, A. *Environ. Sci. Technol.* **2000**, *34*, 659−662.
(13) Zhang, Z.; Xiang, Q.; Glatt, H.; Platt, K. L.; Goldstein, B. D.; Witz, G. *Free Radicals Biol. Medicine* **1995**, *18*(3), 411−419.
(14) Jonsson, M.; Lind, J.; Reitberger, T.; Eriksen, T. E.; Merényi, G. *J. Phys. Chem. A* **1993**, *97*, 8229−8233.
(15) Lei, L.; Hu, X.; Yue, P. L.; Bossmann, S. H.; Göb, S.; Braun, A. M. *J. Photochem. Photobiol., A: Chem.* **1998**, *116*, 159−166.
(16) Wang, G.; Hsieh, S.; Hong, C. *Water Res.* **2000**, *34*, 3882−3887.
(17) Poon, C. S.; Huang, Q.; Fung, P. C. *Chemosphere* **1999**, *38*, 1005−1014.
(18) Shu, H.; Huang, C.; Hang, M. *Chemosphere* **1994**, *29*, 2597−2607.
(19) Mack, J.; Bolton, J. R. *J. Photochem. Photobiol., A: Chem.* **1999**, *128*, 1−13.
(20) Glaze, W. H.; Lay, Y.; Kang, J. W. *Ind. Eng. Chem. Res.* **1995**, *34*, 2314−2323.
(21) Crittenden, J. C.; Shumin, H.; Hand, D. W.; Green, S. A. *Water Res.* **1999**, *33*, 2315−2328.
(22) Simic, M. The chemistry of peroxy radicals and its implication to radiation biology. In *Fast Proceses in Radiation Chemistry and Biology*; Adams, E., Fielden, E.; Michael, B., Eds.; Wiley: 1975; pp 162−179.
(23) Getoff, N. Peroxyl radicals in the treatment of waste solutions. In *Peroxyl Radicals*; Wiley: 1997.
(24) Nadezhdin, A. D.; Dunford, H. B. *Can. J. Chem.* **1979**, *57*, 3017−3022.
(25) Nadezhdin, A. D.; Dumford, H. B. *J. Phys. Chem.* **1979**, *83*(15), 1957−1961.
(26) Tang, Y.; Thorn, R. P.; Mauldin, R. L., III; Wine, P. H. *J. Photochem. Photobiol. A. Chem.* **1988**, *44*, 243−258.
(27) Ferraudi, G. *Elements of Inorganic Photochemistry*; Wiley: 1988.
(28) Braun, A. M.; Maurette, M. T.; Oliveros, E. *Photochemical Technnology*; Ollis, D. F., Serpone, N., Eds.; Transl., Wiley: 1991.
(29) Bolton, J. R.; Cater, S. R. Homogeneous photodegradation of pollutants in contaminated waters. In *Aquatic and Surface Photochemistry*; Helz, G. R.; Zepp, R. G., Crosby, D. G., Eds.; Lewis Publishers: Boca Raton, FL, 1994; pp 467−490 and references therein.
(30) Lipczynska-Kochany, E.; Bolton, J. R. *J. Photochem. Photobiol. A: Chem.* **1991**, *58*, 315−322.
(31) Ross, A. B.; Mallard, W.; Helman, W. P.; Buxton, G. V.; Huie, R.; Neta, P. *NIST Standard Reference Database: Ver. 3.0;* Notre Dame Radiation Laboratory, IN and National Institute of Standards and Technology: Gaithesburg, MD, 1998.
(32) García Einschlag, F. S.; Capparelli, A. L. *Obra de Software: FILTRO 1.0*; Dirección Nacional del Derecho de Autor, Argentina, Expediente No. 040954, 2000.
(33) Onstein, P.; Stefan, M. I.; Bolton, J. R. *J. Adv. Oxid. Technol.* **1999**, *4*(2), 231−236.
(34) Kochany, J.; Bolton, J. R. *J. Phys. Chem.* **1991**, *95*, 5116−5120.
(35) Wolfrum, E. J.; Ollis, D. F.; Lim, P. K.; Fox, M. A. *J. Photochem. Photobiol. A* **1994**, *78*, 259−265.
(36) Cercek, B.; Ebert, M. *Adv. Chem. Ser.* **1968**, *81*, 210−221.
(37) Neta, P.; Dorfman, L. M. *Adv. Chem. Ser.* **1968**, *81*, 222−230.
(38) Lipczynska-Kochany, E. *Chemosphere* **1991**, *22*, 529−536.
(39) García Einschlag, F. S.; Carlos, L.; Capparelli, A. L.; Oliveros, E.; Braun, A. M. *Photochem. Photobiol. Sci.* **2002**, *1* (7), 520−525.

Received for review November 21, 2001. Revised manuscript received June 21, 2002. Accepted July 8, 2002.

ES0103039